Cancer Cell
Article

Hepatocyte IKKβ/NF-κB Inhibits Tumor Promotion and Progression by Preventing Oxidative Stress-Driven STAT3 Activation

Guobin He,[1,5] Guann-Yi Yu,[1,5] Vladislav Temkin,[1] Hisanobu Ogata,[1] Christian Kuntzen,[1] Toshiharu Sakurai,[1,3] Wolfgang Sieghart,[4] Markus Peck-Radosavljevic,[4] Hyam L. Leffert,[2] and Michael Karin[1,*]
[1]Laboratory of Gene Regulation and Signal Transduction
[2]Hepatocyte Growth Control and Stem Cell Laboratory
School of Medicine, University of California, San Diego, 9500 Gilman Drive, La Jolla, CA 92093, USA
[3]Department of Clinical Molecular Biology, Graduate School of Medicine, Kyoto University, 54 Shogoin Kawahara-cho, Sakyo-ku, Kyoto 606-8507, Japan
[4]Department of Internal Medicine III, Division of Gastroenterology/Hepatology, Medical University of Vienna, Währingergürtel 18-20, 1090 Vienna, Austria
[5]These authors contributed equally to this work
*Correspondence: karinoffice@ucsd.edu
DOI 10.1016/j.ccr.2009.12.048

SUMMARY

The NF-κB activating kinase IKKβ suppresses early chemically induced liver tumorigenesis by inhibiting hepatocyte death and compensatory proliferation. To study IKKβ's role in late tumor promotion and progression, we developed a transplant system that allows initiated mouse hepatocytes to form hepatocellular carcinomas (HCC) in host liver after a long latency. Deletion of IKKβ long after initiation accelerated HCC development and enhanced proliferation of tumor initiating cells. These effects of IKKβ/NF-κB were cell autonomous and correlated with increased accumulation of reactive oxygen species that led to JNK and STAT3 activation. Hepatocyte-specific STAT3 ablation prevented HCC development. The negative crosstalk between NF-κB and STAT3, which is also evident in human HCC, is a critical regulator of liver cancer development and progression.

INTRODUCTION

Carcinogenesis, consisting of initiation, promotion, and progression, is a multistage process governed by cumulative genetic and epigenetic alterations (Nowell, 1976). Tumor initiators induce genetic changes that cause proto-oncogene activation and/or loss of tumor suppressors (Hennings et al., 1993). Initiation alone, however, is insufficient for cancer development and tumor promotion is needed for expansion of initiated cells into premalignant lesions that progress into malignant tumor masses. While initiation is brief and irreversible, tumor promotion and progression are long-lasting processes that up to a point may be reversed, thereby providing a rationale for chemointervention. Tumor promotion is thought to depend on an interaction between initiated cells and their microenvironment (Albini and Sporn, 2007) and inflammation is a frequent tumor promoter (Karin, 2006). Through production of proinflammatory cytokines, chemokines, and reactive oxygen species (ROS), the inflammatory microenvironment exerts a constant evolutionary pressure on initiated cells while supporting their proliferation and expansion (Coussens and Werb, 2002). Relative to early tumor promotion, the mechanisms that control tumor progression and malignant conversion are poorly understood. An improved understanding of these late steps in the tumorigenic process is of great importance as it has been estimated that most individuals harbor premalignant lesions that

Significance

HCC, a leading cause of cancer-related deaths, develops after long latency in the context of viral hepatitis or obesity. While much is known about early etiologic events in HCC development, little is known about mechanisms governing progression of premalignant lesions to overt carcinomas. We developed a physiologically relevant transplant system for studying malignant progression of chemically induced HCC. Using this system we found that in addition to its established effect on hepatocyte survival during early tumor induction, IKKβ-driven NF-κB suppresses malignant progression by preventing accumulation of reactive oxygen species that can lead to activation of STAT3, an oncogenic transcription factor that is critical for HCC development. An inverse correlation between NF-κB and STAT3 was also found in a major subfraction of human HCC.

never or rarely progress to full blown neoplasms (Boucher and Yakovlev, 1997).

One of the slowest cancers to appear and grow is hepatocellular carcinoma (HCC), the third leading cause of cancer-related death worldwide (Parkin et al., 2001). HCC usually appears after exposure to liver carcinogens or infection with one of two hepatitis viruses, HBV or HCV, but its evolution and growth may take more than 30 years (Bosch et al., 2004; Tong et al., 1995). HCC frequently develops in the context of hepatosteatosis and liver cirrhosis following chronic liver damage due to oxidative and endoplasmic reticulum stress, accompanied by inflammation that drives the compensatory proliferation of surviving hepatocytes (El-Serag and Rudolph, 2007; Parekh and Anania, 2007; Wang and Weinman, 2006). Cirrhotic livers contain premalignant lesions ranging from dysplastic foci to dysplastic hepatocyte nodules (Wanless, 1995). These lesions are more proliferative than the surrounding parenchyma and resemble early HCC (Hytiroglou et al., 2007). A small number of these lesions undergo malignant conversion, whose rate may be accelerated by environmental factors (Seki et al., 2000; Takayama et al., 1990). Premalignant lesions are also found in chemically induced rodent models of HCC (Pitot, 1990), but their conversion into frank HCC is controversial (Sell and Leffert, 2008). Understanding the molecular mechanisms underlying the progression and malignant conversion of premalignant lesions is critical for any effort to slow down or prevent HCC development. However, animal models for studying HCC progression are scarce.

In contrast, early steps in the molecular etiology of HCC have been extensively studied using transgenic or chemically induced mouse HCC models (Calvisi and Thorgeirsson, 2005; Fausto, 1999). Using the chemical procarcinogen diethylnitrosamine (DEN) to induce HCC in mice, we made the initially surprising discovery that hepatocyte-specific ablation of the IKKβ subunit of the IκB kinase (IKK) complex dramatically enhances HCC induction (Maeda et al., 2005). These findings stand in marked contrast to the outcome of IKKβ deletion in enterocytes, which prevents development of colitis associated cancer (CAC) (Greten et al., 2004). Yet, in both HCC and CAC, deletion of IKKβ in myeloid cells (Kupffer cells in the liver and lamina propria macrophages and dendritic cells in the colon) attenuates tumor development due to reduced expression of tumor-promoting cytokines (Greten et al., 2004; Grivennikov et al., 2009; Maeda et al., 2005). The anti-tumorigenic activity of hepatocyte IKKβ was suggested to be due to induction of NF-κB-dependent pro-survival and antioxidant genes. Indeed, DEN administration to hepatocyte IKKβ-deficient ($Ikk\beta^{\Delta hep}$) mice results in elevated ROS accumulation, hepatocyte death, and compensatory proliferation, all of which are prevented by the antioxidant butylated hydroxyanisole (BHA) (Kamata et al., 2005; Maeda et al., 2005). Similar findings were obtained in mice lacking the NEMO/IKKγ regulatory subunit ($Nemo/Ikk\gamma^{\Delta hep}$ mice), whose hepatocyte-specific ablation results in spontaneous liver damage, hepatosteatosis, fibrosis, and HCC development, which are all preventable by BHA administration (Luedde et al., 2007). In contrast, in other mouse models of HCC that depend on chronic inflammation and not on liver damage and death-driven compensatory proliferation, hepatocyte IKKβ and NF-κB were found to promote tumor development (Haybaeck et al., 2009; Pikarsky et al., 2004). Under such conditions, NF-κB activation in hepatocytes is needed for expression of chemokines and cytokines that organize and maintain an inflammatory microenvironment.

Although DEN administration activates IKK transiently and does not lead to chronic hepatitis (Maeda et al., 2005), DEN-induced HCC (dih) depends on production of the NF-κB-regulated cytokine IL-6 by resident Kupffer cells (Naugler et al., 2007; Sakurai et al., 2008). In this case, Kupffer cells are activated by IL-1α released by dying hepatocytes and the absence of parenchymal IKKβ enhances IL-6 production. Interestingly, male mice produce more IL-6 upon DEN administration than females, and this accounts for the marked male bias in HCC induction (Naugler et al., 2007). Although it remains to be established whether differential IL-6 production accounts for the gender bias in human HCC, a recent epidemiological study identified elevated serum IL-6 as a critical and reliable predictor of progression from HBV-induced hepatitis to HCC (Wong et al., 2009). Elevated IL-6 also correlates with accelerated progression from HCV-induced hepatitis to HCC especially in women (Nakagawa et al., 2009), which produce more IL-6 after menopause (Cioffi et al., 2002). The postmenopausal increase in IL-6 production may explain the delayed onset of HCC in women relative to men (Chen et al., 2006). IL-6 transduces its signals via a heterodimeric receptor composed of the cytokine-binding IL-6R subunit and the gp130 signaling subunit (Kamimura et al., 2003). Recently, activating gp130 mutations were identified as the causal event in nonmalignant hepatic adenomas (Rebouissou et al., 2009). These mutations activate the Ras-MAPK pathway and STAT3, an oncogenic transcription factor that is critical for CAC development (Bromberg and Wang, 2009; Grivennikov et al., 2009).

To further dissect the molecular mechanisms that govern liver carcinogenesis, here we examine the role of IKKβ-driven NF-κB in HCC progression as well as its relationships with STAT3 in both dih in mice and human clinical specimens.

RESULTS

A Transplant System for Studying Progression/Malignant Conversion of Initiated Hepatocytes

To dissociate initiation and early tumor promotion from HCC progression and malignant conversion, we established an experimental system for studying late events that affect hepatocarcinogenesis. We treated C57BL/6 mice with DEN at 15 days of age and waited for 3 months to allow hepatocyte initiation and clonal expansion. At that point, hepatocytes were isolated and transplanted via splenic injection into livers of MUP-uPA transgenic mice (Figure 1A). The latter overexpress urokinase-type plasminogen activator (uPA) in their hepatocytes and are therefore subjected to low-grade but continuous liver damage and regeneration, making them ideal recipients for exogenous hepatocytes (Weglarz et al., 2000). Furthermore, MUP-uPA mice develop mild liver fibrosis but no HCC by 8 months of age (Figure S1A, available online). Their livers also exhibit elevated expression of IL-6 mRNA (Figure S1B) and enhanced ROS accumulation (Figure S1C). All of these changes resemble the microenvironment within which human liver cancer forms. Within a month, transplanted hepatocytes marked with green fluorescent protein (GFP) formed small islands in the recipient's liver

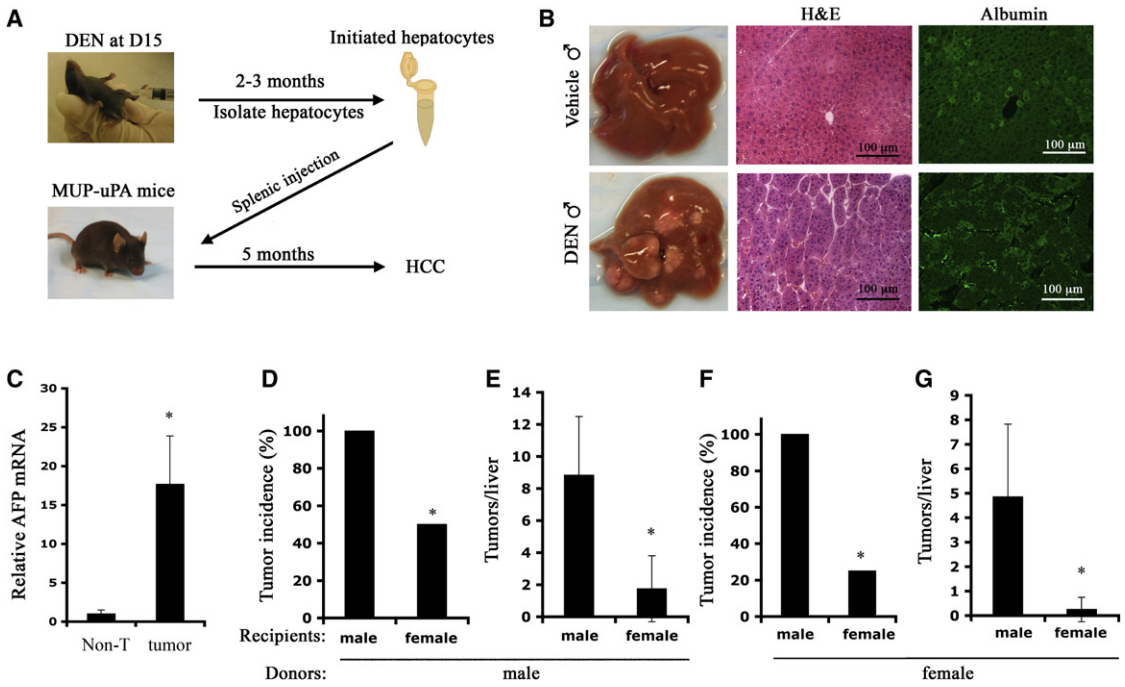

Figure 1. A Transplant System for Studying HCC Progression

(A) A diagram of experimental protocol. C57BL/6 pups were given a single i.p. injection of DEN (25 mg/kg) when 15 days old. Hepatocytes were isolated 2–3 months later and transplanted into 3-week-old MUP-uPA mice via intrasplenic injection. Recipients were sacrificed 5 months later for liver tumor analysis.

(B) Representative livers of male MUP-uPA mice 5 months after transplantation with hepatocytes from vehicle- or DEN-treated male mice. Liver sections were stained with H&E and albumin antibody. Scale bars represent 100 μm.

(C) Relative expression of α-fetoprotein mRNA was determined by real-time PCR in liver tumors (tumor) and surrounding nontumor liver (Non-T). n = 4; *$p < 0.01$ by t test.

(D–G) DEN-treated male (D and E) or female mice (F and G) were used as hepatocyte donors to MUP-uPA recipients of the indicated gender. Tumor incidence (D and F) and multiplicity (E and G)were determined at 5 months after transplantation. n = 8–10 for each group; *$p < 0.01$ by t test (E and G) or *$p < 0.01$ by chi-square test (D and F). Error bars represent SD. See also Figure S1.

but otherwise were barely distinguishable from host hepatocytes (Figure S1D). By 5 months after transplantation, male MUP-uPA mice receiving hepatocytes from DEN-initiated males developed multiple tumor nodules that were absent in mice receiving hepatocytes from vehicle-injected mice (Figure 1B) or in untransplanted MUP-uPA mice (data not shown). The tumors, which exhibited a typical trabecular HCC structure and expressed albumin and elevated amounts of the HCC marker α-fetoprotein (AFP; Figures 1B and 1C), are likely to be derived from the transplanted DEN-initiated cells. The latter failed to grow in normal C57BL/6 mice (data not shown), suggesting that the MUP-uPA liver microenvironment is conducive and essential for conversion of initiated hepatocytes into HCC.

To further characterize this system and determine its physiological relevance, we examined whether the host gender affects HCC formation by transplanted hepatocytes. We injected male and female mice with DEN and transplanted their hepatocytes into MUP-uPA hosts of either gender. Five months later, male recipients of male hepatocytes exhibited at least one HCC per liver, whereas less than 50% of female recipients of male hepatocytes bore tumors (Figure 1D). Furthermore, tumor multiplicity was five times higher in male hosts (Figure 1E). Even more striking results were obtained with transplanted female hepatocytes (Figures 1F and 1G). Although fewer tumors were seen in this case, consistent with the gender bias in HCC induction (Naugler et al., 2007), male hosts of initiated female hepatocytes exhibited 4-fold higher tumor incidence and nearly 20 times higher tumor multiplicity than female hosts of female hepatocytes (Figures 1F and 1G). Since MUP-uPA expression is similar between males and females (Weglarz et al., 2000; data not shown), these data demonstrate that gender plays a critical role not only in HCC initiation and early promotion but also in tumor progression. Removing initiated hepatocytes from the female microenvironment where they hardly progress into HCC to a male microenvironment results in a substantial enhancement of HCC development. These findings support the physiological relevance of the transplant system.

Deletion of *Ikkβ* in Initiated Hepatocytes Enhances Tumorigenic Potential

Next we examined whether the IKKβ-NF-κB pathway, which inhibits DEN-induced (Maeda et al., 2005) and spontaneous (Luedde et al., 2007) HCC development, most likely by suppressing death-driven compensatory proliferation that occurs during early tumor promotion (Karin, 2006), also affects progression. To this end, we gave $Ikk\beta^{f/f}$ male mice, which express normal amounts of IKKβ, DEN and transferred their initiated hepatocytes into MUP-uPA mice. After 1 month, male and female hosts were

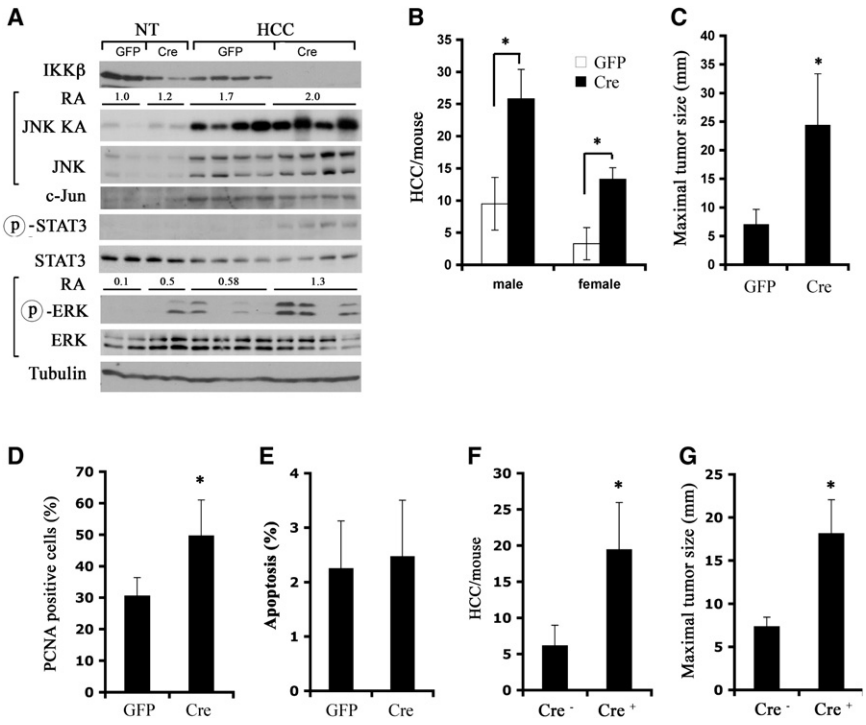

Figure 2. IKKβ Deletion after Initiation Enhances HCC Formation and Growth

(A–C) *Ikkβ*$^{f/f}$ male pups were DEN initiated and used as hepatocyte donors into MUP-uPA mice. IKKβ in transplanted hepatocytes was deleted 1 month later by injection of Adv-Cre. Adv-GFP was used as a control. Mice were sacrificed 4 months later and whole-cell lysates were prepared from dissected HCCs and surrounding nontumor livers (NT).

(A) Lysates were gel separated and immunoblotted with the indicated antibodies or used for measurement of JNK kinase activity by immune-complex kinase assay. Relative JNK kinase activity (KA) and ERK phosphorylation in the different samples were determined by densitometry and the average relative activities (RA) for each group of samples are indicated.

(B and C) HCCs per liver were counted (B) and maximal tumor size was measured (C). n = 7–10 for each group; *p < 0.05.

(D and E) Tumor cell proliferation and apoptosis were determined by PCNA (D) and TUNEL (E) staining, respectively, of paraffin-embedded liver sections (n = 10 for each group; *p < 0.05).

(F and G) *Ikkβ*$^{f/f}$ (Cre^{-}) and *Ikkβ*$^{f/f}$/*Mx1-Cre* (Cre^{+}) DEN-initiated males were used as hepatocyte donors to male MUP-uPA recipients. IKKβ deletion was accomplished by poly(IC) injection 1 month after transplantation. HCC multiplicity (F) and maximal sizes (G) were determined 4 months later (n = 10 for each group; *p < 0.01). Error bars represent SD. See also Figure S2.

injected with GFP- or Cre-expressing adenoviruses (Adv) to delete *Ikkβ* in transplanted hepatocytes. Adv infection caused mild liver injury, indicated by a small elevation in circulating ALT (Figure S2). Administration of Adv-Cre induced efficient IKKβ deletion (Figure 2A) and resulted in a 3- to 4-fold increase in tumor multiplicity and size in both male and female recipients relative to Adv-GFP infection (Figures 2B and 2C). These results are consistent with the previous observation that inactivation of IKKβ in cultured hepatocytes enhances their proliferation (Koch et al., 2009).

In addition to complete IKKβ deletion, Adv-Cre administration increased STAT3 and ERK phosphorylation in HCCs relative to Adv-GFP administration (Figure 2A). However, JNK and c-Jun expression and JNK kinase activity, which were elevated in HCCs relative to non-tumor liver tissue, did not show large differences between IKKβ-expressing and non-expressing HCCs. *Ikkβ*-deleted HCCs contained more proliferating (PCNA-positive) cells than IKKβ-expressing tumors (Figure 2D), but the rate of HCC apoptosis was not affected by the IKKβ status (Figure 2E).

As an alternative approach to delete *Ikkβ* after tumor initiation, we used DEN-initiated *Ikkβ*$^{f/f}$/*Mx1-Cre* mice as hepatocyte donors. These mice express Cre recombinase from the interferon-inducible *Mx1* promoter (Kuhn et al., 1995), such that administration of the interferon inducer poly(IC) results in efficient *Ikkβ* deletion in liver (Maeda et al., 2005). Using this experimental setup, we deleted *Ikkβ* 1 month after transplantation. This resulted in a large increase in HCC multiplicity and size in hosts receiving initiated hepatocytes from *Ikkβ*$^{f/f}$/*Mx1-Cre* donors relative to hosts transplanted with *Ikkβ*$^{f/f}$ hepatocytes (Figures 2F and 2G). These results clearly demonstrate that in addition to enhancing tumor initiation and/or early promotion, deletion of *Ikkβ* in initiated hepatocytes augments and/or accelerates HCC progression.

Ikkβ Deletion Enhances Hepatosphere Formation and Tumorigenic Potential

To further examine cell-autonomous effects of IKKβ in malignant hepatocytes, we cultured dih from *Ikkβ*$^{f/f}$ mice. Initially, HCC cells failed to proliferate and gradually died in standard hepatocyte culture medium (data not shown). Addition of phenobarbital, a liver tumor promoter (Kaufmann et al., 1988), and EGF overcame this problem and allowed the derivation of several cell strains from dih. Three of the strains (dih10–12) expressed both albumin and AFP, consistent with being derived from AFP-expressing HCCs (Figure S3A). All dih cells were albumin positive, suggesting little contamination, if any, with non-parenchymal cells (Figure S3B). These cells showed increased PCNA expression and enhanced STAT3 phosphorylation relative to primary hepatocytes, but did not exhibit an obvious increase in gp130 or β-catenin phosphorylation under standard culture conditions (Figure S3C). Infection of dih cells with Adv-Cre resulted in nearly complete *Ikkβ* deletion (*Ikkβ*$^{\Delta}$) (Figure 3A). *Ikkβ*$^{\Delta}$ dih cells grew in multilayers and formed spheroids even under non-confluent conditions, while *Ikkβ*$^{f/f}$ dih cells mainly grew as monolayers (Figure S3D). When plated onto Petri dishes without serum, *Ikkβ*$^{f/f}$ dih cells formed a few floating spheroids (hepatospheres) that could be passaged in culture to yield secondary hepatospheres (Figure 3A). Interestingly, *Ikkβ*$^{\Delta}$ dih cells formed

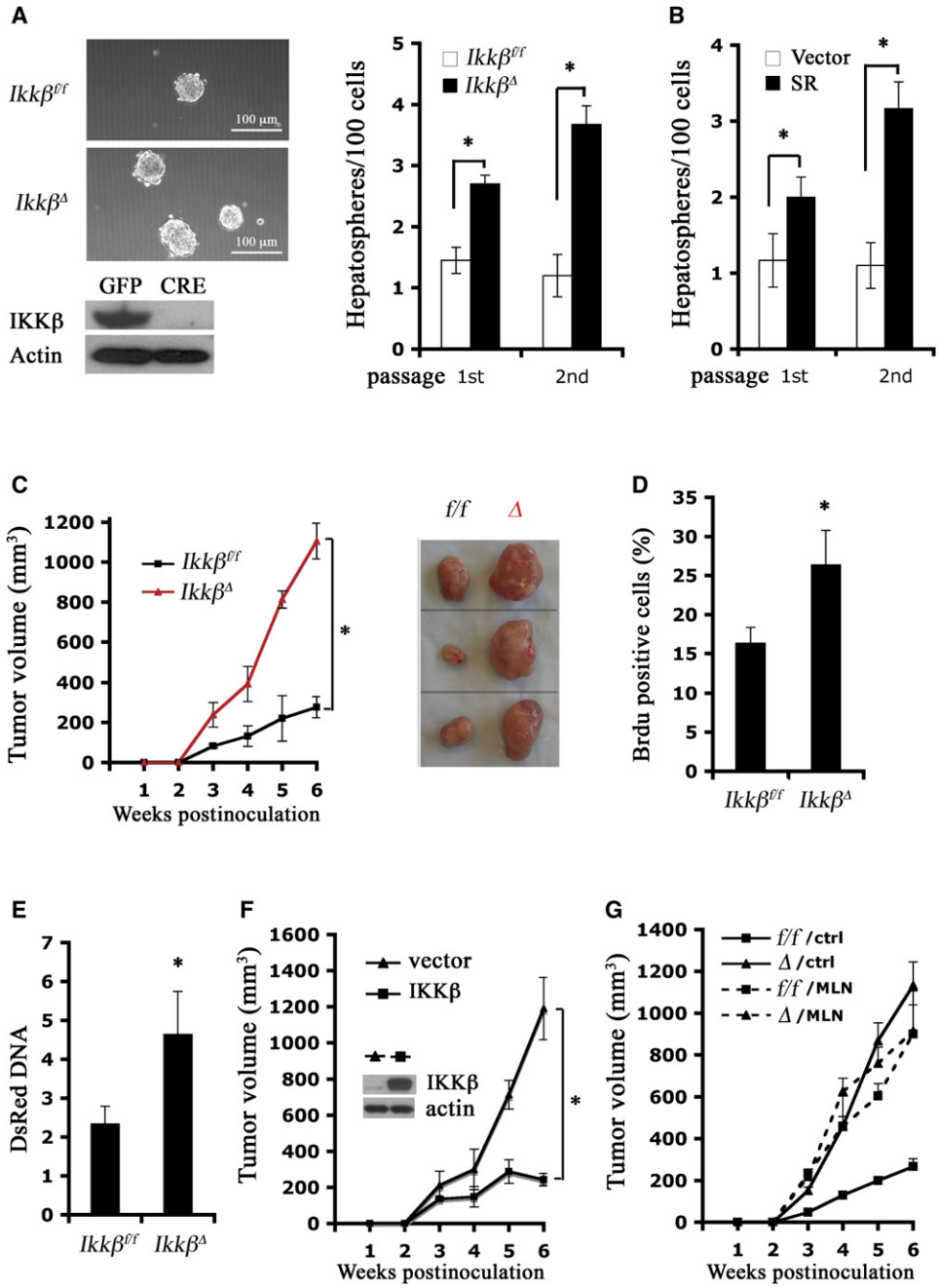

Figure 3. IKKβ Deletion in Initiated Cells Enhance Proliferation and Self-Renewal of HCC Progenitors

(A) dih cell strains from *Ikkβ*$^{f/f}$ mice were cultured and infected with Adv-GFP or Adv-Cre. Whole-cell lysates of infected dih10 cells were immunoblotted for IKKβ (bottom panel). The cells were further cultured without serum on Petri dishes to form hepatospheres (top panels). Numbers of 1° and 2° hepatospheres formed per 100 plated cells were determined (n = 3; *p < 0.05). Scale bars represent 100 μm.

(B) *Ikkβ*$^{f/f}$ dih10 cells were infected with an empty retrovirus (vector) or a retrovirus expressing IκBα super-repressor (SR). Stably transfected cells were selected and cultured as above and hepatosphere formation was analyzed (n = 3; *p < 0.05).

(C and D) IKKβ-expressing (*Ikkβ*$^{f/f}$) and -deficient (*Ikkβ*$^{\Delta}$) dih10 cells (2.5 × 10^6 each) were s.c. injected into 8-week-old C57BL/6 mice.

(C) Allograft volume was measured weekly (n = 5; *p < 0.01). Dissected tumors are shown on the right.

(D) BrdU incorporation into tumors was determined (n = 5; *p < 0.05).

(E) *Ikkβ*$^{f/f}$ and *Ikkβ*$^{\Delta}$ dih12 cells were labeled with dsRed and 4 × 10^5 cells were seeded into MUP-uPA mouse livers. Relative amounts of dsRed DNA in transplanted MUP-uPA livers were determined by real-time PCR 3 weeks after inoculation and normalized to actin DNA as a measurement of cell growth (n = 5; *p < 0.05).

(F) *Ikkβ*$^{\Delta}$ dih10 cells were reconstituted with a control vector or wild-type IKKβ expression vector and were s.c. injected into 8-week-old C57BL/6 mice. Allograft volume was measured weekly (n = 5; *p < 0.01).

(G) *Ikkβ*$^{f/f}$ and *Ikkβ*$^{\Delta}$ dih10 cells were s.c. injected as above. Starting from day 2, mice were treated daily with MLN120B or vehicle by oral gavage. Tumor volume was measured weekly (n = 5; p < 0.01, f/f/control versus f/f/MLN by one-way ANOVA). Error bars represent SD. See also Figure S3.

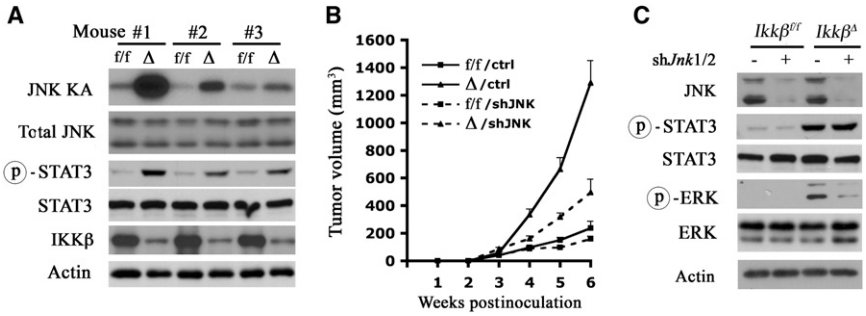

Figure 4. STAT3 Is Activated in the Absence of IKKβ Independently of JNK

(A) Tumors derived from *Ikkβ*$^{f/f}$ (f/f) and *Ikkβ*^{Δ} (Δ) dih10 cells were collected and lysed. Tumor lysates were examined for JNK kinase activity (KA) and STAT3 phosphorylation.

(B and C) *Ikkβ*$^{f/f}$ and *Ikkβ*^{Δ} dih10 cells were infected with lentiviruses expressing either a control shRNA (control) or shRNAs against mouse *Jnk1/2* (sh*Jnk1/2*) and implanted s.c.

(B) Tumor growth was measured (n = 5; $p < 0.05$, Δ/control versus Δ/sh*Jnk1/2* by one-way ANOVA).

(C) Tumors were collected and lysed. Lysates were examined for expression and phosphorylation of the indicated proteins. Error bars represent SD. See also Figure S4.

twice as many primary hepatospheres and 3-fold more secondary hepatospheres than *Ikkβ*$^{f/f}$ dih cells. Transduction of *Ikkβ*$^{f/f}$ dih cells with an IκB super-repressor lentivirus (Boehm et al., 2007) also enhanced hepatosphere formation (Figure 3B), suggesting that IKKβ inhibits hepatosphere formation via NF-κB.

In mammary cancer, spheroid-forming cells were suggested to be tumor progenitors (Al-Hajj and Clarke, 2004). To test whether *Ikkβ* deletion in dih cells enhances tumorigenic potential, we subcutaneously implanted *Ikkβ*$^{f/f}$ and *Ikkβ*^{Δ} dih10 cells into C57BL/6 mice. *Ikkβ*^{Δ} cells grew more quickly than *Ikkβ*$^{f/f}$ cells and after 6 weeks formed tumors that were four times larger than those formed by *Ikkβ*$^{f/f}$ cells (Figure 3C) and had higher proliferative index (Figure 3D). A similar difference in proliferative potential between *Ikkβ*$^{f/f}$ and *Ikkβ*^{Δ} dih cells was seen when the cells were grown in the liver microenvironment: dsRed-labeled *Ikkβ*^{Δ} dih12 cells formed faster growing HCCs in MUP-uPA livers than *Ikkβ*$^{f/f}$ dih12 cells (Figure 3E). Conversely, retroviral-mediated reconstitution of IKKβ in *Ikkβ*^{Δ} dih10 cells suppressed tumorigenic growth (Figure 3F). Thus, the effect of *Ikkβ* deletion on hepatoma growth is reversible. Enhanced tumorigenic growth of subcutaneously inoculated dih10 cells was also seen upon treatment of tumor-bearing mice with the specific IKKβ inhibitor MLN120B (Wen et al., 2006). MLN120B enhanced tumorigenic growth of *Ikkβ*$^{f/f}$ dih cells and not *Ikkβ*^{Δ} cells and its effect was equivalent to that of *Ikkβ* deletion (Figure 3G). These data demonstrate that IKKβ is an inhibitor of HCC growth and progression and suggest that its effect is direct and not due to irreversible genetic alterations.

STAT3 Activity Is Elevated in the Absence of IKKβ Because of ROS-Mediated SHP1/2 Inactivation

To determine how loss of IKKβ accelerates tumor growth and progression, we examined its effect on signaling pathways that affect hepatocyte proliferation. Subcutaneous tumors formed by *Ikkβ*^{Δ} dih cells exhibited a tendency toward higher JNK activity, but the effect was variable (Figure 4A). A more consistent change was increased STAT3 phosphorylation in *Ikkβ*^{Δ} dih tumors. Despite the variable effect of IKKβ on JNK activity in HCCs and subcutaneous tumors, silencing of JNK1/2 expression in dih10 cells suppressed their tumorigenic growth (Figure 4B) and the inhibitory effect was greater in *Ikkβ*^{Δ} cells. Curiously, silencing of JNK1/2 expression decreased ERK phosphorylation in *Ikkβ*^{Δ} tumors, but had no effect on STAT3 phosphorylation (Figure 4C).

We examined the cause of elevated STAT3 activity in *Ikkβ*^{Δ} dih cells. In vitro, both IL-6 and IL-22, which are major STAT3 activators in liver (Naugler et al., 2007; Zenewicz et al., 2007), led to higher STAT3 activity in *Ikkβ*^{Δ} dih cells than in *Ikkβ*$^{f/f}$ dih cells (Figures S4A and S4B). Conversely, expression of constitutively active IKKβ (IKKβ^{EE}) in *Ikkβ*^{Δ} dih cells inhibited IL-6-induced STAT3 activation (Figure S4C). The IKKβ inhibitor MLN120B also enhanced IL-6-induced STAT3 activation in dih cells and a human liver cancer cell line (Figure S4D). Enhancement of STAT3 activation required a 24–48 hr preincubation with MLN120B, suggesting that IKKβ regulates STAT3 indirectly. No obvious differences in IL-6 or IL-22 expression were detected between IKKβ-expressing and non-expressing HCCs (Figure S4E).

Given these results, we considered that increased STAT3 activity in *Ikkβ*^{Δ} dih cells is due to a cell intrinsic effect on the STAT3 signaling pathway. In support of this, phosphorylation of JAK2, a Janus kinase involved in IL-6-mediated STAT3 activation (Kamimura et al., 2003), was enhanced in tumors formed by *Ikkβ*^{Δ} dih cells relative to *Ikkβ*$^{f/f}$ dih tumors (Figure 5A), suggesting that elevated STAT3 activation in *Ikkβ*^{Δ} dih cells is the consequence of enhanced JAK2 activity. Indeed, inhibition of JAK2 expression by shRNA reduced IL-6-induced STAT3 activation in both *Ikkβ*$^{f/f}$ and *Ikkβ*^{Δ} dih cells (Figure S5A). We also examined other regulators of the JAK2-STAT3 pathway. Expression of SOCS3, a critical feedback inhibitor of cytokine signaling and a STAT3 target gene (Auernhammer et al., 1999; Brender et al., 2001), whose ablation enhances HCC development (Ogata et al., 2006), was elevated in IKKβ-deficient tumors (Figure 5A). SOCS3 upregulation is likely to be transcriptional because SOCS3 mRNA was also higher in the absence of IKKβ (Figure S5B). Thus, enhanced JAK2 activation cannot be due to diminished SOCS3 expression as previously found in the hypothalamus (Zhang et al., 2008).

Other negative regulators of JAK2-STAT3 signaling include the SH2-containing phosphatases, SHP1 and SHP2 (Valentino and Pierre, 2006). Tumors derived from dih cells expressed higher amounts of SHP2 than SHP1, but these were not significantly affected by IKKβ (Figure 5A). However, both SHP1 and SHP2 phosphatase activities were significantly lower in tumors formed by *Ikkβ*^{Δ} dih cells relative to *Ikkβ*$^{f/f}$ dih tumors (Figure 5B). SHP1 and SHP2 activities in *Ikkβ*^{Δ} tumors were restored upon reconstitution with IKKβ (Figure S5C). To validate a role for SHP1/2 in regulation of STAT3, we overexpressed SHP2, the more

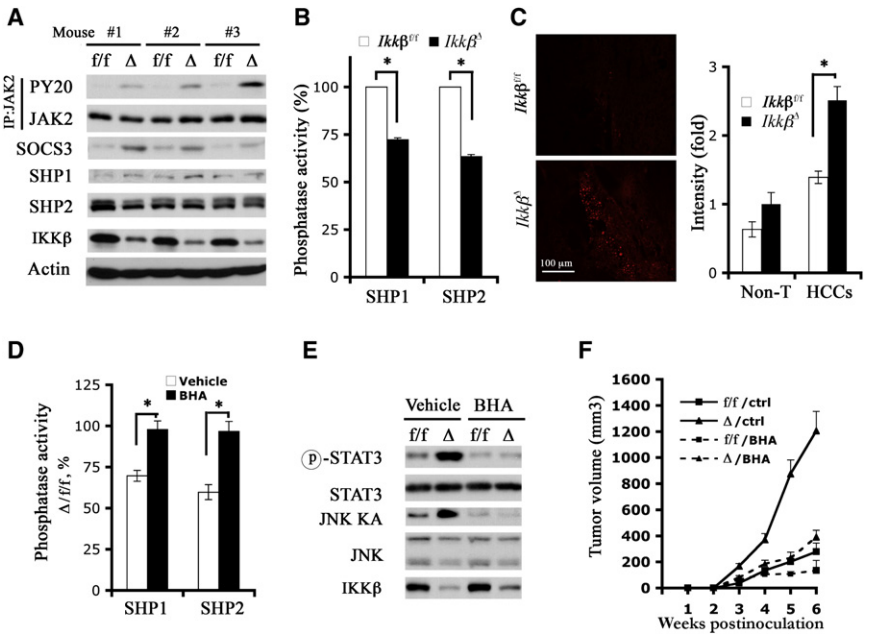

Figure 5. ROS-Mediated SHP1/2 Inhibition in IKKβ-Deficient HCCs Correlates with STAT3 Activation and Accelerated Tumor Growth

(A) Tumors derived from *Ikkβ*$^{f/f}$ (f/f) and *Ikkβ*^{Δ} (Δ) dih10 cells were collected and lysed. Tumor lysates were immunoprecipitated with an anti-JAK2 antibody and examined for JAK2 tyrosine phosphorylation with PY20 antibody. Tumor lysates were also used for immunoblot analyses with the indicated antibodies.

(B) SHP1 and SHP2 were immunoprecipitated from the above tumor lysates and their phosphatase activities were measured (n = 4; *p < 0.05).

(C) Fresh frozen sections of HCCs from transplanted MUP-uPA mice were analyzed for superoxide accumulation by dihydroethydine staining. Fluorescence intensity in several fields was quantitated by ImageJ and relative average increases in fluorescent intensity are shown (n = 3; *p < 0.01). The scale bar represents 100 μm.

(D–F) *Ikkβ*$^{f/f}$ (f/f) and *Ikkβ*^{Δ} (Δ) dih10 cells, 2.5 × 10^6 each, were s.c. implanted into 8-week-old C57BL/6 mice. Starting on day 2, the mice were switched to a diet containing vehicle or BHA (0.7%) for 6 weeks.

(D) Tumors were collected from BHA-treated and untreated mice and lysed and SHP1/2 phosphatase activities were measured. The data were plotted as SHP1/2 phosphatase activities in *Ikkβ*^{Δ} tumors relative to activities in *Ikkβ*$^{f/f}$ tumors (n = 4; *p < 0.05).

(E) Tumor lysates were used for determining JNK kinase activity and STAT3 phosphorylation.

(F) Tumor volume was measured weekly (n = 5; p < 0.01, Δ/ctrl versus Δ/BHA by one way ANOVA). Error bars represent SD. See also Figure S5.

abundant of the two phosphatases in HCC cells, and this resulted in a strong inhibition of IL-6-induced STAT3 phosphorylation in both *Ikkβ*$^{f/f}$ and *Ikkβ*^{Δ} dih cells (Figure S5D). These results strongly suggest that reduced SHP1/2 activities in IKKβ-deficient HCCs are responsible for the elevated STAT3 activation.

SHP1 and SHP2 are members of the protein tyrosine phosphatase (PTP) family (Figure S5E), whose catalytic cysteine is highly susceptible to oxidation (Meng et al., 2002; Salmeen et al., 2003). Several PTPs are subject to reversible inactivation in response to growth factor (Meng et al., 2002) or cytokine-induced ROS and this inactivation is potentiated in the absence of NF-κB (Kamata et al., 2005). We therefore examined ROS accumulation in HCCs and in dih cells. Staining with the ROS (superoxide) indicator dihydroethydine revealed more ROS accumulation in HCCs relative to surrounding tissue and IKKβ-deficient HCCs stained stronger than IKKβ-expressing HCCs (Figure 5C). Cultured *Ikkβ*^{Δ} dih cells also accumulated more ROS both under basal culture conditions and in response to IL-6 or EGF than *Ikkβ*$^{f/f}$ dih cells and this was reversed by expression of constitutively active IKKβ^{EE} (Figures S5F and S5G). To examine the role of ROS in reduced SHP1/2 activities and STAT3 upregulation in IKKβ-deficient HCCs, we fed tumor-bearing mice with BHA, a potent antioxidant (Maeda et al., 2005). BHA feeding completely restored SHP1/2 phosphatase activities and reduced JNK activity and STAT3 phosphorylation in tumors formed by *Ikkβ*^{Δ} dih cells to levels comparable to those in *Ikkβ*$^{f/f}$ tumors (Figures 5D and 5E). Importantly, BHA consumption reduced *Ikkβ*^{Δ} tumor growth to a level that was similar to that of *Ikkβ*$^{f/f}$ tumors in untreated mice (Figure 5F). Collectively, these data suggest that ROS accumulation in IKKβ-deficient HCCs is responsible for reduced PTP activity, JNK and STAT3 activation, as well as accelerated tumor growth.

STAT3 Activity Is Required for HCC Formation and Growth

To examine the contribution of activated STAT3 to the enhanced tumorigenic potential of *Ikkβ*^{Δ} dih cells, we treated tumor-bearing mice with AG490, an inhibitor of STAT3 phosphorylation (Eriksen et al., 2001). AG490 inhibited the growth of *Ikkβ*^{Δ} subcutaneous tumors and had a more modest effect on *Ikkβ*$^{f/f}$ tumorigenic growth (Figure S6A). Immunoblot analysis verified that AG490 inhibited STAT3 phosphorylation regardless of IKKβ status (Figure S6B). A similar effect on tumor growth was observed with another STAT3 inhibitor, S3I-201 (Figure S6C), which inhibits STAT3 activation through binding to its SH2 domain (Siddiquee et al., 2007). S3I-201 also inhibited STAT3 phosphorylation (Figure S6D). To more specifically address the role of STAT3, we silenced its expression in dih cells via lentiviral expression of a STAT3-specific shRNA (Figure S6E). In sharp contrast to cells transduced with a control lentivirus encoding scrambled shRNA that formed subcutaneous tumors, dih cells transduced with the STAT3 shRNA failed to grow into subcutaneous tumors regardless of their IKKβ status (Figure 6A).

To further examine the role of STAT3 in HCC development, we administered DEN to 15-day-old hepatocyte-specific STAT3-deficient mice (*Stat3*$^{f/f}$/*Alb-Cre* mice = *Stat3*^{Δhep}) (Figure 6B). *Stat3*^{Δhep} mice were markedly resistant to dih development with more than 6-fold reduction in HCC multiplicity relative to *Stat3*$^{f/f}$ mice (Figure 6C). Tumors in *Stat3*^{Δhep} mice, which retained their STAT3 deficiency (Figure 6B), were also

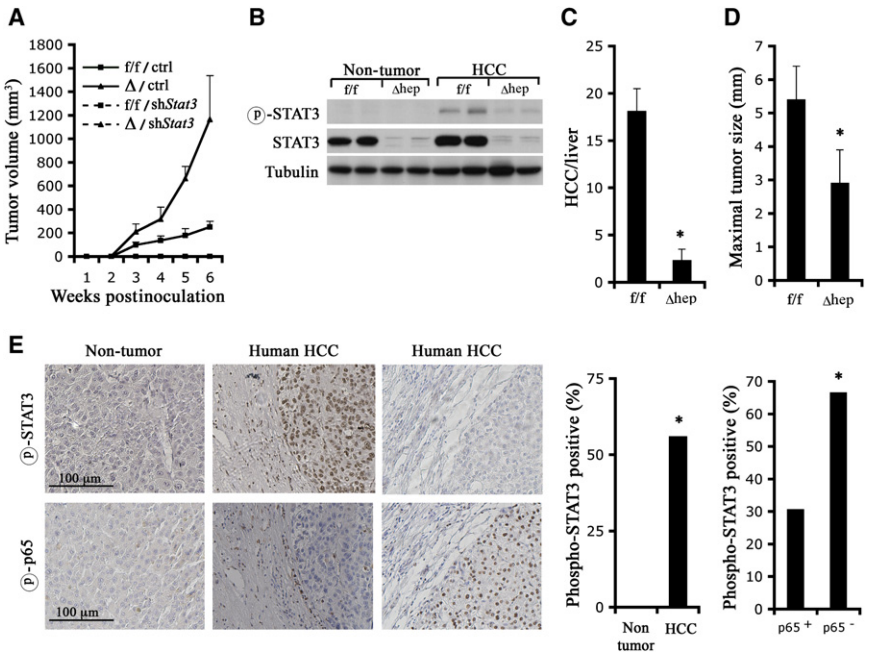

Figure 6. STAT3 Is Required for HCC Formation and Growth

(A) *Ikkβ*$^{f/f}$ (f/f) and *Ikkβ*^{Δ} (Δ) dih10 cells were infected with lentiviruses expressing either scrambled shRNA (ctrl) or an shRNA against mouse *Stat3* (sh*Stat3*). Stably transfected cells were selected and 2.5 × 10^6 cells were s.c. implanted. Tumor growth was measured (n = 5; $p < 0.01$, f/f/ctrl versus f/f /shSTAT3; $p < 0.01$, Δ/ctrl versus Δ/shSTAT3 by one-way ANOVA).

(B–D) *Stat3*$^{f/f}$ and *Stat3*^{Δhep} male mice were injected with 25 mg/kg DEN when 15 days old. Mice were sacrificed 8 months later and HCC induction was evaluated.

(B) HCCs and surrounding non-tumor tissues were collected and lysed and STAT3 expression and phosphorylation were examined.

(C and D) Tumor multiplicity (n = 10; *$p < 0.01$) (C) and maximal tumor sizes (n = 10; *$p < 0.05$) (D) were determined.

(E) STAT3 and NF-κB activation in human HCC. The top panels show representative samples of nontumor liver tissue and liver tissue containing HCC were stained with a phospho-STAT3 antibody. The bottom panels show adjacent parallel sections of the same samples shown in the top panels were stained with a phospho-p65 antibody. The bar graphs present the frequency of phospho-STAT3-positive HCC specimens among all HCCs or among p65-positive and p65-negative HCCs (*$p < 0.05$ by chi-square analysis). Error bars represent SD. See also Figure S6 and Table S1.

significantly smaller than HCCs in *Stat3*$^{f/f}$ mice (Figure 6D). We derived *Stat3*$^{f/f}$ dih cells from dih of *Stat3*$^{f/f}$ mice, but deletion of STAT3 from these cells by Ad-Cre infection resulted in inhibition of cell growth and induction of cell death (Figures S6F and S6G). These data strongly suggest that STAT3 is required for mouse HCC development, growth, and survival.

We also examined the status of STAT3 activation in more than 50 different human HCC specimens and found that nearly 60% of them exhibited activated nuclear STAT3, which could not be detected in non-tumor liver tissue from the same patient (Figure 6E). As observed previously (Calvisi et al., 2006), STAT3 activation was more pronounced in the more aggressive tumors (Table S1). We also found that 25% (13/52) of human HCCs were positive for phospho-p65/RelA, an indicator of NF-κB activation. However, phospho-p65-positive HCCs were often negative for activated STAT3. Only 30.8% of phospho-p65-positive HCCs were positive for activated STAT3, whereas 66.7% of phospho-p65-negative HCCs exhibited activated STAT3 (Figure 6E). These data show that a major subfraction of human HCCs exhibits an inverse relationship between NF-κB and STAT3.

DISCUSSION

We have developed an experimental system based on transplantation of DEN-initiated hepatocytes into MUP-uPA mouse liver that allows one to examine factors and mechanisms that affect the progression of initiated, preneoplastic hepatocytes into full-blown HCC. Using this system, we found that loss of IKKβ in initiated hepatocytes greatly enhances HCC development even when IKKβ is deleted or inhibited many months after tumor initiation. Previously, IKKβ and its regulatory subunit NEMO/IKKγ were found to negatively control HCC development in models that depend on compensatory proliferation triggered by chemically induced or spontaneous hepatocyte death and liver injury (Luedde et al., 2007; Maeda et al., 2005). This inhibitory effect on HCC development was proposed to be exerted during early tumor promotion and be due to loss of NF-κB pro-survival activity, which is more severe in *Nemo/Ikkγ*^{Δhep} than in *Ikkβ*^{Δhep} mice (Karin, 2006). The current results, however, show that IKKβ-driven NF-κB also inhibits late tumor promotion and progression of initiated hepatoma cells through effects on ROS metabolism that exert a negative control over the STAT3 signaling pathway (Figure 7). STAT3 itself is frequently activated in human HCCs, especially in aggressive tumors with poor prognosis (Calvisi et al., 2006; Table S1) and we now show that STAT3 activation is subject to negative regulation by NF-κB and is essential for HCC induction. The inverse relationship between NF-κB and STAT3 also applies to a major subfraction of human HCCs.

The ability to temporally and physically separate tumor initiation, which in our case occurs upon DEN-induced mutagenesis, from late tumor promotion and malignant progression has been instrumental to the success of this study. Interestingly, transplantation of DEN-initiated hepatocytes from either a male or female donor to normal C57BL/6 recipients, as opposed to MUP-uPA mice, has never given rise to detectable HCCs. These findings underscore the importance of the microenvironment and circulatory system in tumor progression and malignant conversion. Although the exact factors responsible for the permissive nature of the MUP-uPA liver microenvironment remain to be determined, it should be noted that MUP-uPA mice experience chronic low grade liver injury accompanied by a small, but significant, elevation in IL-6 expression and ROS

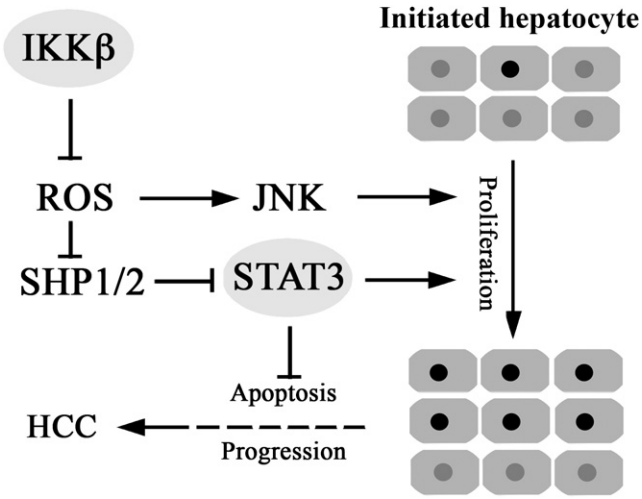

Figure 7. A Central Role for IKKβ and ROS-Controlled STAT3 Signaling in HCC Development

Inactivation of IKKβ or other antioxidant defenses in hepatocytes favors ROS accumulation and leads to oxidative inhibition of PTPs, including SHP1 and SHP2. This results in activation of JNK and STAT3, which stimulate the proliferation of initiated preneoplastic hepatocytes. This contributes both to early tumor promotion and HCC progression. In addition, STAT3 activation suppresses apoptosis in progressing HCCs.

accumulation and eventually develop low grade liver fibrosis. These are the same kind of changes that accompany the development of human HCC.

Using the transplant system, as well as a culture system that allowed the derivation of the dih cell strains described above, we found that deletion or inhibition of IKKβ in initiated hepatocytes or HCC-derived cells increases their proliferative and tumorigenic potential. The effect is due to loss of NF-κB activity, because specific NF-κB inhibition through expression of IκB super-repressor results in a similar effect. Similar findings were made in squamous cell carcinoma, where NF-κB was shown to inhibit keratinocyte proliferation and Ras-induced tumorigenesis through negative regulation of JNK activity, whose exact mechanism was not identified (Dajee et al., 2003; Zhang et al., 2004). We now show that another way through which NF-κB inhibits proliferation and tumorigenesis is negative regulation of STAT3 activation. As shown previously for JNK in TNF-α-treated NF-κB-deficient cells (Kamata et al., 2005), enhanced STAT3 activation in $Ikk\beta^{\Delta}$ cells or tumors is due to oxidative inhibition of PTPs, whose catalytic cysteine is extremely susceptible to oxidation (Meng et al., 2002; Salmeen et al., 2003). While previous work has shown that PTPs are oxidatively inactivated under rather harsh conditions that favor ROS accumulation, such as TNF-α-induced cell death (Kamata et al., 2005), the present work shows that significant PTP inhibition and subsequent kinase activation occur under relatively normal conditions, as long as NF-κB-dependent antioxidant defenses (Kamata et al., 2005; Pham et al., 2004) are dismantled. The antioxidant function of NF-κB, which is exerted in part through expression of ferritin heavy chain and superoxide dismutase 2 (Kamata et al., 2005; Pham et al., 2004), is particularly important in the liver, an organ that is heavily engaged in oxidative metabolism. Indeed, the deletion of hepatocyte NEMO/IKKγ results in spontaneous liver damage, hepatosteatosis, fibrosis, and HCC formation, all of which can be prevented by administration of an antioxidant (Luedde et al., 2007).

Although our work demonstrates an essential and critical role for STAT3 in HCC development and progression, STAT3 has been known to be critically involved in several other malignancies, including squamous cell carcinoma (Chan et al., 2004) and CAC (Bollrath et al., 2009; Grivennikov et al., 2009) and JAK2 or STAT3 inhibitors were found to inhibit the growth of several human cancers (Hedvat et al., 2009). Notably, we detected phosphorylated (i.e., activated) STAT3 in approximately 60% of human HCCs, with STAT3-positive tumors being more aggressive. These findings are consistent with those of other studies in which STAT3 was found to be activated in the majority of HCCs with poor prognosis and not in surrounding non-tumor tissue or normal liver (Calvisi et al., 2006; Lin et al., 2009). Expression of the STAT3-activating cytokine IL-6 is elevated in both liver cirrhosis and HCC (Tilg et al., 1992; Trikha et al., 2003) and was recently found to correlate with rapid progression from viral hepatitis to HCC (Nakagawa et al., 2009; Wong et al., 2009). In addition, activating mutations in the gene encoding the gp130 signaling subunit for IL-6 and other cytokine receptors were found to account for benign hepatic adenomas (Rebouissou et al., 2009). When combined with a β-catenin activating mutation, these mutations, which result in STAT3 activation lead to HCC development. Our findings suggest that NF-κB may also be engaged in negative regulation of STAT3 in a subfraction of human HCCs as the frequency of STAT3-positive HCCs is 2-fold lower in NF-κB-positive HCCs than in NF-κB-negative HCCs. Altogether, there is little doubt that STAT3 is a key regulator of liver tumorigenesis in mice and men. Our results suggest that in addition to its role in early tumor development, where it suppresses apoptosis and enhances proliferation of preneoplastic cells (Bromberg and Wang, 2009), STAT3 plays a critical role during tumor progression when it is activated many months after the HCC-initiating event caused by DEN exposure. We identified the IKK-NF-κB axis as a negative regulator of STAT3 activation, but it needs to be determined how NF-κB activity is downregulated during human hepatocarcinogenesis and it is necessary to evaluate its relative contribution to STAT3 activation vis-a-vis the effects of cytokines and growth factors. We also show that STAT3 can be activated in response to ROS accumulation and it should be noted that several of the most prominent HCC risk factors, including HCV and hepatosteatosis, result in oxidative stress (El-Serag and Rudolph, 2007; Parekh and Anania, 2007; Wang and Weinman, 2006).

The present work as well as previous work with $Ikk\beta^{\Delta hep}$ and $Nemo/Ikk\gamma^{\Delta hep}$ mice (Luedde et al., 2007; Maeda et al., 2005; Sakurai et al., 2006) demonstrate an anti-tumorigenic role for NF-κB in hepatocytes. However, it was also described that NF-κB activation promotes hepatocarcinogenesis in $Mdr2^{-/-}$ mice, which develop cholestatic hepatitis and eventually liver cancer (Pikarsky et al., 2004), and in transgenic mice, which overexpress lymphotoxin αβ in their liver (Haybaeck et al., 2009). Notably in both $Mdr2^{-/-}$ and $LT\alpha\beta$ -transgenic mice, HCC development depends on chronic low-grade inflammation and no liver injury has been observed either prior to or

subsequent to NF-κB inhibition (Haybaeck et al., 2009; Pikarsky et al., 2004). Most likely, in these models, in contrast to the injury-driven $Ikk\beta^{\Delta hep}$+DEN and $Nemo/Ikk\gamma^{\Delta hep}$ models, the main function of NF-κB in hepatocytes is to upregulate the expression of chemokines needed for recruitment of inflammatory cells that contribute to the microenvironment in which these tumors develop. In the $Nemo/Ikk\gamma^{\Delta hep}$ model, however, the absence of hepatocyte NF-κB results in ROS accumulation and its sequela, chronic liver damage, hepatosteatosis, fibrosis, and eventual HCC development, whereas in the transplantation model described above IKKβ-deficient and -proficient initiated HCC cells are placed into a permissive microenvironment created by chronic proteolytic damage to the liver. In human hepatocarcinogenesis, which is mainly caused and promoted by chronic HCV or HBV infections or by hepatosteatosis, both inflammatory and injury/repair responses are likely to be involved (Berasain et al., 2009). In addition, some viruses inhibit NF-κB activation to facilitate cell killing and avoid immune detection (Roulston et al., 1999). Therefore, all of the above model systems bear some relevance to human HCC development, and, given the complex effects of IKK/NF-κB inhibition, a more attractive and likely candidate for therapeutic targeting is the STAT3 signaling pathway.

EXPERIMENTAL PROCEDURES

Mice and HCC Induction

$Ikk\beta^{f/f}$ mice (Park et al., 2002) were backcrossed into the C57BL/6 background for at least six generations. $Ikk\beta^{f/f}$/*Mx1-Cre* mice were described previously (Maeda et al., 2005). MUP-uPA transgenic mice were kindly provided by E.P. Sandgren, University of Wisconsin-Madison (Weglarz et al., 2000). $Stat3^{\Delta hep}$ mice were obtained from D.E. Levy at New York University (Lee et al., 2002). For HCC induction, 15-day-old littermates were injected with 25 mg/kg DEN (Sigma). DEN-injected mice were sacrificed either 3 months after DEN injection to be used as hepatocyte donors or maintained for 8 months to monitor HCC development. All mouse experimental protocols were approved by the University of California San Diego Animal Care Program, following National Institutes of Health guidelines. Histology, gene expression, and cell signaling were analyzed as described previously (Maeda et al., 2005; Sakurai et al., 2008).

Isolation and Transplantation of Primary Hepatocytes

Primary hepatocytes were isolated from DEN-treated mice as described previously (Leffert et al., 1979). For transplantation, cell preparations with viability greater than 80% were used. Three-week-old MUP-uPA transgenic mice received 1.2×10^5 viable hepatocytes in 30 μl PBS via intrasplenic injection with a 30-G needle (Weglarz et al., 2000). Transplanted mice were sacrificed 5 months later to monitor HCC development. For deletion of $Ikk\beta$ in transplanted hepatocytes, mice were given 10^9 pfu of Adv-GFP or Adv-Cre via the tail vein 1 month after transplantation. Alternatively, $Ikk\beta^{f/f}$/*Mx1-Cre* hepatocytes were transplanted as above and the recipients were given three injections (250 μg each) of poly(IC) every other day one month after hepatocyte transplantation.

Human HCC Specimens and Their Analysis

Human HCC specimens were from the Department of Internal Medicine, Division of Gastroenterology/Hepatology, Medical University of Vienna. HCC samples were obtained during liver transplantation from a total of 52 patients (49 males and 3 females) who had no prior therapy before surgery (Sieghart et al., 2006). None of the patients was diagnosed with regional lymph node metastasis and only one patient had distal metastasis at the time of liver transplantation. Sections prepared from paraffin-embedded blocks were stained with either phospho-STAT3 antibody (Cell Signaling) or phospho-p65 antibody (Cell Signaling) at a dilution of 1:50. Conditions for use of all antibodies have been posted to http://biorating.com. Positive nuclear staining was scored as follows: ***, large area staining; **, staining of multiple smaller areas; *, staining of scattered few positive cells. Immunohistochemical staining of HCC specimens as well as retrospective clinical data collection and analysis were approved by the local ethics committee of the Medical University of Vienna.

Statistical Analysis

Data are presented as means ± SD. Differences in means were analyzed by Student's t test and one-way ANOVA. Tumor incidence (%) was analyzed by chi-square analysis. p values < 0.05 were considered significant.

Additional experimental procedures are available in the Supplemental Information.

SUPPLEMENTAL INFORMATION

Supplemental Information includes six figures, one table, and Supplemental Experimental Procedures and can be found with this article online at doi:10.1016/j.ccr.2009.12.048.

ACKNOWLEDGMENTS

We thank David Levy for providing $Stat3^{\Delta hep}$ mice. G.H. was supported by a postdoctoral fellowship from Damon Runyon Cancer Research Foundation and G.Y.Y was supported by an American Diabetes Association Postdoctoral research grant to M.K. V.T., H.O., and C.K. were supported by Arthritis Foundation Research Fellowship, Kanzawa Medical Research Foundation, and American Institute for Cancer Research Fellowship, respectively. Research was supported by grants from the National Institutes of Health (ES006376, CA113602, and CA118165) and the Superfund Basic Research Program (P42ES010337). M.K. is an American Cancer Society Research Professor.

Received: September 4, 2009
Revised: December 17, 2009
Accepted: February 3, 2010
Published: March 15, 2010

REFERENCES

Al-Hajj, M., and Clarke, M.F. (2004). Self-renewal and solid tumor stem cells. Oncogene *23*, 7274–7282.

Albini, A., and Sporn, M.B. (2007). The tumour microenvironment as a target for chemoprevention. Nat. Rev. Cancer *7*, 139–147.

Auernhammer, C.J., Bousquet, C., and Melmed, S. (1999). Autoregulation of pituitary corticotroph SOCS-3 expression: characterization of the murine SOCS-3 promoter. Proc. Natl. Acad. Sci. USA *96*, 6964–6969.

Berasain, C., Castillo, J., Perugorria, M.J., Latasa, M.U., Prieto, J., and Avila, M.A. (2009). Inflammation and liver cancer. Ann. NY Acad. Sci. *1155*, 206–221.

Boehm, J.S., Zhao, J.J., Yao, J., Kim, S.Y., Firestein, R., Dunn, I.F., Sjostrom, S.K., Garraway, L.A., Weremowicz, S., Richardson, A.L., et al. (2007). Integrative genomic approaches identify IKBKE as a breast cancer oncogene. Cell *129*, 1065–1079.

Bollrath, J., Phesse, T.J., von Burstin, V.A., Putoczki, T., Bennecke, M., Bateman, T., Nebelsiek, T., Lundgren-May, T., Canli, O., Schwitalla, S., et al. (2009). gp130-mediated Stat3 activation in enterocytes regulates cell survival and cell-cycle progression during colitis-associated tumorigenesis. Cancer Cell *15*, 91–102.

Bosch, F.X., Ribes, J., Diaz, M., and Cleries, R. (2004). Primary liver cancer: worldwide incidence and trends. Gastroenterology *127*, S5–S16.

Boucher, K.M., and Yakovlev, A.Y. (1997). Estimating the probability of initiated cell death before tumor induction. Proc. Natl. Acad. Sci. USA *94*, 12776–12779.

Brender, C., Nielsen, M., Kaltoft, K., Mikkelsen, G., Zhang, Q., Wasik, M., Billestrup, N., and Odum, N. (2001). STAT3-mediated constitutive expression of SOCS-3 in cutaneous T-cell lymphoma. Blood *97*, 1056–1062.

Bromberg, J., and Wang, T.C. (2009). Inflammation and cancer: IL-6 and STAT3 complete the link. Cancer Cell *15*, 79–80.

Calvisi, D.F., and Thorgeirsson, S.S. (2005). Molecular mechanisms of hepatocarcinogenesis in transgenic mouse models of liver cancer. Toxicol. Pathol. *33*, 181–184.

Calvisi, D.F., Ladu, S., Gorden, A., Farina, M., Conner, E.A., Lee, J.S., Factor, V.M., and Thorgeirsson, S.S. (2006). Ubiquitous activation of Ras and Jak/Stat pathways in human HCC. Gastroenterology *130*, 1117–1128.

Chan, K.S., Sano, S., Kiguchi, K., Anders, J., Komazawa, N., Takeda, J., and DiGiovanni, J. (2004). Disruption of Stat3 reveals a critical role in both the initiation and the promotion stages of epithelial carcinogenesis. J. Clin. Invest. *114*, 720–728.

Chen, C.H., Huang, G.T., Yang, P.M., Chen, P.J., Lai, M.Y., Chen, D.S., Wang, J.D., and Sheu, J.C. (2006). Hepatitis B- and C-related hepatocellular carcinomas yield different clinical features and prognosis. Eur. J. Cancer *42*, 2524–2529.

Cioffi, M., Esposito, K., Vietri, M.T., Gazzerro, P., D'Auria, A., Ardovino, I., Puca, G.A., and Molinari, A.M. (2002). Cytokine pattern in postmenopause. Maturitas *41*, 187–192.

Coussens, L.M., and Werb, Z. (2002). Inflammation and cancer. Nature *420*, 860–867.

Dajee, M., Lazarov, M., Zhang, J.Y., Cai, T., Green, C.L., Russell, A.J., Marinkovich, M.P., Tao, S., Lin, Q., Kubo, Y., and Khavari, P.A. (2003). NF-kappaB blockade and oncogenic Ras trigger invasive human epidermal neoplasia. Nature *421*, 639–643.

El-Serag, H.B., and Rudolph, K.L. (2007). Hepatocellular carcinoma: epidemiology and molecular carcinogenesis. Gastroenterology *132*, 2557–2576.

Eriksen, K.W., Kaltoft, K., Mikkelsen, G., Nielsen, M., Zhang, Q., Geisler, C., Nissen, M.H., Ropke, C., Wasik, M.A., and Odum, N. (2001). Constitutive STAT3-activation in Sezary syndrome: tyrphostin AG490 inhibits STAT3-activation, interleukin-2 receptor expression and growth of leukemic Sezary cells. Leukemia *15*, 787–793.

Fausto, N. (1999). Mouse liver tumorigenesis: models, mechanisms, and relevance to human disease. Semin. Liver Dis. *19*, 243–252.

Greten, F.R., Eckmann, L., Greten, T.F., Park, J.M., Li, Z.W., Egan, L.J., Kagnoff, M.F., and Karin, M. (2004). IKKbeta links inflammation and tumorigenesis in a mouse model of colitis-associated cancer. Cell *118*, 285–296.

Grivennikov, S., Karin, E., Terzic, J., Mucida, D., Yu, G.Y., Vallabhapurapu, S., Scheller, J., Rose-John, S., Cheroutre, H., Eckmann, L., and Karin, M. (2009). IL-6 and Stat3 are required for survival of intestinal epithelial cells and development of colitis-associated cancer. Cancer Cell *15*, 103–113.

Haybaeck, J., Zeller, N., Wolf, M.J., Weber, A., Wagner, U., Kurrer, M.O., Bremer, J., Iezzi, G., Graf, R., Clavien, P.A., et al. (2009). A lymphotoxin-driven pathway to hepatocellular carcinoma. Cancer Cell *16*, 295–308.

Hedvat, M., Huszar, D., Herrmann, A., Gozgit, J.M., Schroeder, A., Sheehy, A., Buettner, R., Proia, D., Kowolik, C.M., Xin, H., et al. (2009). The JAK2 inhibitor AZD1480 potently blocks Stat3 signaling and oncogenesis in solid tumors. Cancer Cell *16*, 487–497.

Hennings, H., Glick, A.B., Greenhalgh, D.A., Morgan, D.L., Strickland, J.E., Tennenbaum, T., and Yuspa, S.H. (1993). Critical aspects of initiation, promotion, and progression in multistage epidermal carcinogenesis. Proc. Soc. Exp. Biol. Med. *202*, 1–8.

Hytiroglou, P., Park, Y.N., Krinsky, G., and Theise, N.D. (2007). Hepatic precancerous lesions and small hepatocellular carcinoma. Gastroenterol. Clin. North Am. *36*, 867–887.

Kamata, H., Honda, S., Maeda, S., Chang, L., Hirata, H., and Karin, M. (2005). Reactive oxygen species promote TNFalpha-induced death and sustained JNK activation by inhibiting MAP kinase phosphatases. Cell *120*, 649–661.

Kamimura, D., Ishihara, K., and Hirano, T. (2003). IL-6 signal transduction and its physiological roles: the signal orchestration model. Rev. Physiol. Biochem. Pharmacol. *149*, 1–38.

Karin, M. (2006). Nuclear factor-kappaB in cancer development and progression. Nature *441*, 431–436.

Kaufmann, W.K., Ririe, D.G., and Kaufman, D.G. (1988). Phenobarbital-dependent proliferation of putative initiated rat hepatocytes. Carcinogenesis *9*, 779–782.

Koch, K.S., Maeda, S., He, G., Karin, M., and Leffert, H.L. (2009). Targeted deletion of hepatocyte Ikkbeta confers growth advantages. Biochem. Biophys. Res. Commun. *380*, 349–354.

Kuhn, R., Schwenk, F., Aguet, M., and Rajewsky, K. (1995). Inducible gene targeting in mice. Science *269*, 1427–1429.

Lee, C.K., Raz, R., Gimeno, R., Gertner, R., Wistinghausen, B., Takeshita, K., DePinho, R.A., and Levy, D.E. (2002). STAT3 is a negative regulator of granulopoiesis but is not required for G-CSF-dependent differentiation. Immunity *17*, 63–72.

Leffert, H.L., Koch, K.S., Moran, T., and Williams, M. (1979). Liver cells. Methods Enzymol. *58*, 536–544.

Lin, L., Amin, R., Gallicano, G.I., Glasgow, E., Jogunoori, W., Jessup, J.M., Zasloff, M., Marshall, J.L., Shetty, K., Johnson, L., et al. (2009). The STAT3 inhibitor NSC 74859 is effective in hepatocellular cancers with disrupted TGF-beta signaling. Oncogene *28*, 961–972.

Luedde, T., Beraza, N., Kotsikoris, V., van Loo, G., Nenci, A., De Vos, R., Roskams, T., Trautwein, C., and Pasparakis, M. (2007). Deletion of NEMO/IKK-gamma in liver parenchymal cells causes steatohepatitis and hepatocellular carcinoma. Cancer Cell *11*, 119–132.

Maeda, S., Kamata, H., Luo, J.L., Leffert, H., and Karin, M. (2005). IKKbeta couples hepatocyte death to cytokine-driven compensatory proliferation that promotes chemical hepatocarcinogenesis. Cell *121*, 977–990.

Meng, T.C., Fukada, T., and Tonks, N.K. (2002). Reversible oxidation and inactivation of protein tyrosine phosphatases in vivo. Mol. Cell *9*, 387–399.

Nakagawa, H., Maeda, S., Yoshida, H., Tateishi, R., Masuzaki, R., Ohki, T., Hayakawa, Y., Kinoshita, H., Yamakado, M., Kato, N., et al. (2009). Serum IL-6 levels and the risk for hepatocarcinogenesis in chronic hepatitis C patients An analysis based on gender differences. Int. J. Cancer *125*, 2264–2269.

Naugler, W.E., Sakurai, T., Kim, S., Maeda, S., Kim, K., Elsharkawy, A.M., and Karin, M. (2007). Gender disparity in liver cancer due to sex differences in MyD88-dependent IL-6 production. Science *317*, 121–124.

Nowell, P.C. (1976). The clonal evolution of tumor cell populations. Science *194*, 23–28.

Ogata, H., Kobayashi, T., Chinen, T., Takaki, H., Sanada, T., Minoda, Y., Koga, K., Takaesu, G., Maehara, Y., Iida, M., and Yoshimura, A. (2006). Deletion of the SOCS3 gene in liver parenchymal cells promotes hepatitis-induced hepatocarcinogenesis. Gastroenterology *131*, 179–193.

Parekh, S., and Anania, F.A. (2007). Abnormal lipid and glucose metabolism in obesity: implications for nonalcoholic fatty liver disease. Gastroenterology *132*, 2191–2207.

Park, J.M., Greten, F.R., Li, Z.W., and Karin, M. (2002). Macrophage apoptosis by anthrax lethal factor through p38 MAP kinase inhibition. Science *297*, 2048–2051.

Parkin, D.M., Bray, F.I., and Devesa, S.S. (2001). Cancer burden in the year 2000. The global picture. Eur. J. Cancer *37* (*Suppl 8*), S4–S66.

Pham, C.G., Bubici, C., Zazzeroni, F., Papa, S., Jones, J., Alvarez, K., Jayawardena, S., De Smaele, E., Cong, R., Beaumont, C., et al. (2004). Ferritin heavy chain upregulation by NF-kappaB inhibits TNFalpha-induced apoptosis by suppressing reactive oxygen species. Cell *119*, 529–542.

Pikarsky, E., Porat, R.M., Stein, I., Abramovitch, R., Amit, S., Kasem, S., Gutkovich-Pyest, E., Urieli-Shoval, S., Galun, E., and Ben-Neriah, Y. (2004). NF-kappaB functions as a tumour promoter in inflammation-associated cancer. Nature *431*, 461–466.

Pitot, H.C. (1990). Altered hepatic foci: their role in murine hepatocarcinogenesis. Annu. Rev. Pharmacol. Toxicol. *30*, 465–500.

Rebouissou, S., Amessou, M., Couchy, G., Poussin, K., Imbeaud, S., Pilati, C., Izard, T., Balabaud, C., Bioulac-Sage, P., and Zucman-Rossi, J. (2009). Frequent in-frame somatic deletions activate gp130 in inflammatory hepatocellular tumours. Nature *457*, 200–204.

Roulston, A., Marcellus, R.C., and Branton, P.E. (1999). Viruses and apoptosis. Annu. Rev. Microbiol. *53*, 577–628.

Sakurai, T., Maeda, S., Chang, L., and Karin, M. (2006). Loss of hepatic NF-kappa B activity enhances chemical hepatocarcinogenesis through

sustained c-Jun N-terminal kinase 1 activation. Proc. Natl. Acad. Sci. USA *103*, 10544–10551.

Sakurai, T., He, G., Matsuzawa, A., Yu, G.Y., Maeda, S., Hardiman, G., and Karin, M. (2008). Hepatocyte necrosis induced by oxidative stress and IL-1 alpha release mediate carcinogen-induced compensatory proliferation and liver tumorigenesis. Cancer Cell *14*, 156–165.

Salmeen, A., Andersen, J.N., Myers, M.P., Meng, T.C., Hinks, J.A., Tonks, N.K., and Barford, D. (2003). Redox regulation of protein tyrosine phosphatase 1B involves a sulphenyl-amide intermediate. Nature *423*, 769–773.

Seki, S., Sakaguchi, H., Kitada, T., Tamori, A., Takeda, T., Kawada, N., Habu, D., Nakatani, K., Nishiguchi, S., and Shiomi, S. (2000). Outcomes of dysplastic nodules in human cirrhotic liver: a clinicopathological study. Clin. Cancer Res. *6*, 3469–3473.

Sell, S., and Leffert, H.L. (2008). Liver cancer stem cells. J. Clin. Oncol. *26*, 2800–2805.

Siddiquee, K., Zhang, S., Guida, W.C., Blaskovich, M.A., Greedy, B., Lawrence, H.R., Yip, M.L., Jove, R., McLaughlin, M.M., Lawrence, N.J., et al. (2007). Selective chemical probe inhibitor of Stat3, identified through structure-based virtual screening, induces antitumor activity. Proc. Natl. Acad. Sci. USA *104*, 7391–7396.

Sieghart, W., Losert, D., Strommer, S., Cejka, D., Schmid, K., Rasoul-Rockenschaub, S., Bodingbauer, M., Crevenna, R., Monia, B.P., Peck-Radosavljevic, M., and Wacheck, V. (2006). Mcl-1 overexpression in hepatocellular carcinoma: a potential target for antisense therapy. J. Hepatol. *44*, 151–157.

Takayama, T., Makuuchi, M., Hirohashi, S., Sakamoto, M., Okazaki, N., Takayasu, K., Kosuge, T., Motoo, Y., Yamazaki, S., and Hasegawa, H. (1990). Malignant transformation of adenomatous hyperplasia to hepatocellular carcinoma. Lancet *336*, 1150–1153.

Tilg, H., Wilmer, A., Vogel, W., Herold, M., Nolchen, B., Judmaier, G., and Huber, C. (1992). Serum levels of cytokines in chronic liver diseases. Gastroenterology *103*, 264–274.

Tong, M.J., el-Farra, N.S., Reikes, A.R., and Co, R.L. (1995). Clinical outcomes after transfusion-associated hepatitis C. N. Engl. J. Med. *332*, 1463–1466.

Trikha, M., Corringham, R., Klein, B., and Rossi, J.F. (2003). Targeted anti-interleukin-6 monoclonal antibody therapy for cancer: a review of the rationale and clinical evidence. Clin. Cancer Res. *9*, 4653–4665.

Valentino, L., and Pierre, J. (2006). JAK/STAT signal transduction: regulators and implication in hematological malignancies. Biochem. Pharmacol. *71*, 713–721.

Wang, T., and Weinman, S.A. (2006). Causes and consequences of mitochondrial reactive oxygen species generation in hepatitis C. J. Gastroenterol. Hepatol. *21* (*Suppl 3*), S34–S37.

Wanless, I.R. (1995). Terminology of nodular hepatocellular lesions. International Working Party. Hepatology *22*, 983–993.

Weglarz, T.C., Degen, J.L., and Sandgren, E.P. (2000). Hepatocyte transplantation into diseased mouse liver. Kinetics of parenchymal repopulation and identification of the proliferative capacity of tetraploid and octaploid hepatocytes. Am. J. Pathol. *157*, 1963–1974.

Wen, D., Nong, Y., Morgan, J.G., Gangurde, P., Bielecki, A., Dasilva, J., Keaveney, M., Cheng, H., Fraser, C., Schopf, L., et al. (2006). A selective small molecule IkappaB Kinase beta inhibitor blocks nuclear factor kappaB-mediated inflammatory responses in human fibroblast-like synoviocytes, chondrocytes, and mast cells. J. Pharmacol. Exp. Ther. *317*, 989–1001.

Wong, V.W., Yu, J., Cheng, A.S., Wong, G.L., Chan, H.Y., Chu, E.S., Ng, E.K., Chan, F.K., Sung, J.J., and Chan, H.L. (2009). High serum interleukin-6 level predicts future hepatocellular carcinoma development in patients with chronic hepatitis B. Int. J. Cancer *124*, 2766–2770.

Zenewicz, L.A., Yancopoulos, G.D., Valenzuela, D.M., Murphy, A.J., Karow, M., and Flavell, R.A. (2007). Interleukin-22 but not interleukin-17 provides protection to hepatocytes during acute liver inflammation. Immunity *27*, 647–659.

Zhang, J.Y., Green, C.L., Tao, S., and Khavari, P.A. (2004). NF-kappaB RelA opposes epidermal proliferation driven by TNFR1 and JNK. Genes Dev. *18*, 17–22.

Zhang, X., Zhang, G., Zhang, H., Karin, M., Bai, H., and Cai, D. (2008). Hypothalamic IKKbeta/NF-kappaB and ER stress link overnutrition to energy imbalance and obesity. Cell *135*, 61–73.